Mon. Not. R. Astron. Soc. **299,** 305–318 (1998)

Phase-resolved *Hubble Space Telescope* ultraviolet spectroscopy of V795 Her

S. R. Rosen,[1] R. K. Prinja,[2] J. E. Drew,[3] K. O. Mason[4] and S. B. Howell[5]

[1]*Department of Physics and Astronomy, University of Leicester, University Road, Leicester LE1 7RH*
[2]*Department of Physics and Astronomy, University College London, Gower Street, London WC1E 6BT*
[3]*Department of Physics, Imperial College of Science, Technology and Medicine, Prince Consort Road, London SW7 2BZ*
[4]*Mullard Space Science Laboratory, Holmbury St Mary, Dorking, Surrey RH5 6NT*
[5]*Department of Physics and Astronomy, University of Wyoming, PO Box 3905, University Station, Laramie, WY 82071, USA*

Accepted 1997 September 3. Received 1997 May 28

ABSTRACT

We present highly time-resolved *HST* FOS UV spectroscopy of the nova-like binary V795 Her. Several key results emerge. For the first time we find a strong 2.6-h signature in the variability of the UV lines. The *HST* data reveal no evidence of a 4.8-h 'period', in contrast to our previous *IUE* observations. This, and differences in the spectral line characteristics, suggests that *HST* found the system in a different state from earlier *IUE* observations.

The C IV line alone contains a fairly stable, asymmetric, extended blueward absorption trough which we associate with a wind outflow. The 2.6-h variations of the line profiles are largely confined to an interval of about 0.4 in phase and to the velocity regime $-1500 < v < 0\,\mathrm{km\,s^{-1}}$, the changes being dominated by the apparent decline and re-emergence of a blueshifted emission peak. The complex profiles permit many empirical interpretations, but the simplest attributes the variability to a narrow (FWHM$\sim$1000 km s^{-1}) emission component which is always blueshifted with a mean velocity of around –600 km s^{-1}. This interpretation, however, is not readily related to any obvious source within the binary. An alternative picture, which attempts to relate the UV and (simultaneously observed) optical line behaviour, invokes a more stable, broad (FWHM$\sim$2000 km s^{-1}) emission feature, the intrinsic morphology of which is disguised by superposed constant and variable absorption components. One tentative physical explanation of such a decomposition involves an accretion stream that overflows the accretion disc. However, several problems with this model remain to be resolved.

We also draw attention to similarities between the velocity-restricted behaviour in the UV lines of V795 Her and that in the optical lines of T Tauri stars. This might indicate a connection between V795 Her and the magnetically influenced inflow/outflow characteristics associated with the central star in T Tauri systems. If such a connection were eventually demonstrated, it would reopen the question of whether the 2.6-h period in V795 Her is really the binary period and whether the system is in fact related to the intermediate polars.

Key words: accretion, accretion discs – binaries: close – stars: individual: V795 Her – novae, cataclysmic variables – ultraviolet: stars.

1 INTRODUCTION

V795 Her is a member of the nova-like subclass of the cataclysmic variables (CVs), i.e. a close red dwarf–white dwarf binary in which mass is transferred to the compact star through an accretion disc. The nova-like systems are bright, apparently undergoing persistently high levels of accretion. V795 Her has displayed a generally prominent 2.8-h modulation of its optical light curve (e.g. Mironov, Moshkalev & Shugarov 1983; Baidak et al. 1985; Rosen et al. 1989; Kaluzny 1989; Shafter et al. 1990; Zhang et al. 1991), although this may recently have disappeared (Patterson & Skillman 1994; Rosen et al. 1995). It also possesses a distinct 2.6-h radial velocity variation which was proposed as the binary orbital period (Shafter et al. 1990). Whilst this two-period phenomenon was initially used to argue that V795 Her might be an intermediate polar binary containing a magnetized white dwarf, convincing evidence for such a classification remains elusive and indeed, on balance, current data do not favour an intermediate polar interpretation (e.g. Rosen et al.

1995 and references therein; see also van Teeseling, Beuermann & Verbunt 1996). This leaves the original superhump scenario of Zhang et al. (1991) as currently the best explanation of the 2.8-h photometric period. Remarkable, low ($400\,\mathrm{km\,s^{-1}}$) and high ($1500\,\mathrm{km\,s^{-1}}$) velocity amplitude 'S-wave' features have been observed in the Hα emission line of V795 Her (Haswell et al. 1994). Their reconstructed Doppler images of the disc in the Hα and He I λ6678 lines indicated spatially distinct sites for each of the Hα 'S'-wave components and the He I emission. More recent analyses of the optical line profiles in V795 Her have identified two high-amplitude S-wave features, one offset to the blue, the other to the red (Casares et al. 1996; Dickinson et al. 1997). As a result, Casares et al. (1996) resurrected a magnetic model for V795 Her, suggesting that its white dwarf rotates synchronously with the binary. Their model envisages partial disc accretion, nevertheless, and explains the double S-wave behaviour in terms of material entrained in the magnetic field of the white dwarf. This picture is challenged by Dickinson et al. (1997), who prefer a model in which the accretion stream overflows the disc.

V795 Her has also been the subject of an intensive UV (*IUE*) study following the discovery of pronounced, time-dependent morphological changes in its Si IV and C IV lines (Prinja, Rosen & Suppelli 1991, hereafter PRS). Extensive time-resolved *IUE* spectroscopy (Prinja, Drew & Rosen 1992, hereafter PDR; Prinja & Rosen 1993, hereafter PR) found that the UV variation was consistent with periodic behaviour but, extraordinarily, occurred on a period of 4.8 h rather than on either of the known 2.6- and 2.8-h optical periods. The C IV line in particular showed, at certain phases, a P Cygni like profile which is typically associated with mass loss, and was interpreted as reflecting the presence of an outflowing wind in V795 Her. In detail, however, CV wind models then available were unable to account for the pattern of C IV profile variability actually observed. A recently reported *ROSAT* X-ray observation of V795 Her (Rosen et al. 1995) found the 0.1–2.5 keV X-ray flux from the star to be about $5\times10^{-13}\,\mathrm{erg\,s^{-1}\,cm^{-2}}$. These data did not reveal any significant coherent periodic X-ray variability, although a ~15-min quasi-periodic oscillation (QPO)-like variation was seen in both the X-ray and quasi-simultaneous optical data.

In this paper we report on the first ultraviolet observations of V795 Her made with the *Hubble Space Telescope* (*HST*). These observations exploit the enhanced spectral resolution and huge improvement in time resolution possible with *HST*. A parallel study of quasi-simultaneous optical spectroscopy of V795 Her, obtained from the Isaac Newton Telescope, is presented by Dickinson et al. (1997).

2 OBSERVATIONS

Ultraviolet observations of V795 Her were obtained with the COSTAR-corrected *HST* during three closely separated runs in 1994 June. The observations, each spanning an elapsed time of 8.5 h, were obtained between 03:55 and 12:22 UT on 1994 June 20, between 16:54 UT June 21 and 01:22 UT June 22, and between 13:56 and 22:24 UT on June 23. The total on-source exposure amounted to 8.1 h. Data were recorded using the blue digicon with the Faint Object Spectrograph (FOS), operated in RAPID mode to obtain sequences of 20-s exposures with minimal (<1 s) dead time between integrations. A total of 1458 spectra were collected. The source was observed through the 0.9-arcsec aperture and the light dispersed by the G130H grating to obtain spectra covering the 1150–1605 Å spectral range at a resolution of about 1 Å (~230 km s^{-1} at 1300 Å).

For comparison, these observational characteristics represent 6-fold and at least 60-fold improvements in spectral and temporal sampling respectively, relative to our previous *IUE* low-dispersion data. Interruptions owing to Earth occultation, lasting about 40 min in each 96-min satellite orbit, and also occasional passages through the South Atlantic Anomaly, meant that observations of V795 Her were not continuous. The *HST* spectra supplied by STScI were pre-calibrated in both wavelength and flux, with the wavelength scale accurate to about 0.3 Å (~60 km s^{-1} at 1550 Å) (e.g. Bohlin 1995; Dahlem 1995; Koratkar & Evans 1995).

3 THE OVERALL PROPERTIES OF THE UV SPECTRUM

The spectrum that is the mean of all our *HST* data from V795 Her is shown in Fig. 1. All of the prominent lines (e.g. N V λ1240, Si IV λ1400, C IV λ1550), the Si II/Si III/O I blend around 1300 Å and the C II λ1334 line observed in our earlier *IUE* SWP spectra are present in the *HST* data. However, it is now incontestable that the spectrum is also affected by line blanketing (e.g. immediately redward of the C IV line).

To gain some idea of which lines and which parts (if any) of the continuum vary, we have computed a fractional variance spectrum from all the data, i.e.

$$\sigma_\lambda^2 = \frac{1}{(N-1)\bar{f}_\lambda{}^2}\sum_{i=1}^{N}(f_{i\lambda}-\bar{f}_\lambda)^2, \qquad (1)$$

where N is the number of spectra, $f_{i\lambda}$ is the flux at wavelength λ of the ith spectrum and $\bar{f}_\lambda$ is the flux at that wavelength averaged over all spectra. The result is shown in the lower panel of Fig. 1. We point out that statistical noise alone contributes an rms variation of ~13 per cent (variance of 0.017) at wavelengths above 1300 Å, but this rises steeply below 1200 Å owing to the rapid decline in instrumental sensitivity. At 1180 Å the rms variation due to noise is ~35 per cent (variance ~ 0.12).

From Fig. 1 we find that the continuum exhibits a broadly wavelength-independent rms variation of about 20 per cent (or about 15 per cent after removing the noise component). It is obvious, however, that the strong resonance lines dominate the overall variability of the spectra. Variability is also observed in other lines such as C II λ1335 and the blend at 1300 Å. In the Si IV and C IV lines there is a distinct asymmetry to the variance profile with stronger changes on the blue wing of the lines. This may also be true for other lines too, but is not so obvious.

It should be noted that the C IV doublet ($\lambda\lambda$1548.19, $1550.76 - v = 0$, $498\,\mathrm{km\,s^{-1}}$) is not resolved in these data, owing to intrinsic line broadening, while the Si IV doublet components ($\lambda\lambda$1393.76,1402.77 $- v = 0$, 1939 km s^{-1}) are well separated.

3.1 The variability characteristics of the lines and continuum

We have used the 1458 FOS spectra to examine the photometric behaviour of both the line-blanketed 'continuum' and the dominant absorption lines as functions of time. The continuum light curve was generated by summing the flux over three segments of the spectrum devoid of strong absorption features (i.e. $\lambda\lambda$1270–1290, $\lambda\lambda$1310–1330 and $\lambda\lambda$1440–1490). Time-series of the total flux (line plus continuum) in each of the C III, N V, Si IV and C IV lines were also derived. Each time-series was then Fourier analysed.

From the results, plotted in Fig. 2, the key point to emerge is that the lines exhibit a clear variation on a 2.60-h period. Indeed, the

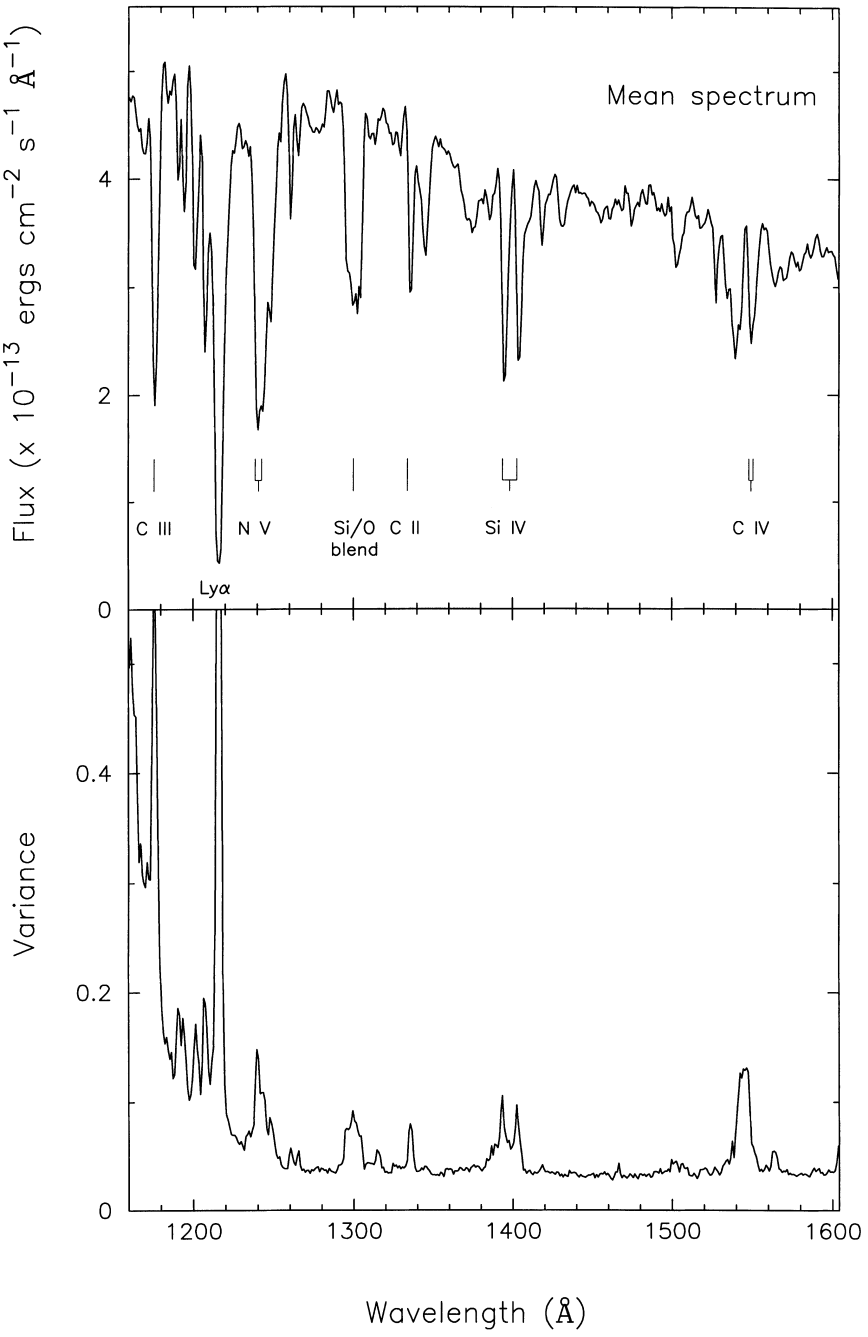

Figure 1. The upper panel shows the mean 1150–1600 Å spectrum of V795 Her measured by the *HST* FOS. The strongest lines are labelled – the tick marks are located at the rest velocity of the particular line. The lower panel shows the corresponding variance spectrum (see Section 3).

largest peak in the power spectrum of each line occurs at the same frequency (9.216 $d^{-1} = 2.60$ h with an uncertainty of typically 0.03 h). The Fourier spectrum of each line also shows notable peaks (and their associated window patterns) at frequencies of $\nu = 24.13\,d^{-1}$ (0.99 h) and 5.7 d^{-1} (4.22 h), features not seen in the power spectrum of the continuum data. These peaks can be identified with the positive and negative sidebands arising from beating of the 2.60-h period with the satellite orbital period [i.e. $P_{\rm beat} = (P_{\rm sat}^{-1} \pm P_{2.6}^{-1})^{-1}$].

In contrast to the lines, the 2.6-h period is not evident in the Fourier spectrum of the continuum flux. It does, however, show excess power between $\nu = 13\,d^{-1}$ (1.8 h) and 18 d^{-1} (1.3 h) which can be decomposed into two overlapping window patterns centred on $\nu = 14.5204$ d^{-1} (1.65 h) and 15.9127 d^{-1} (1.51 h). Nevertheless, in the absence of a more extensive data set, we resist the temptation to claim more periods in this system. The inset in the top panel of Fig. 2 also reveals enhanced power in the frequency range 70–120 d^{-1} (12–21 min) with the most prominent structure within this domain centred around 96 d^{-1} (~15 min). A similar but weaker pattern of power is seen in the Fourier spectra of the lines (not shown). This distribution of power is similar to that reported from the X-ray and optical data (Rosen et al. 1995; see also Zhang et al. 1991 and Shafter et al. 1990). The broad-band nature of the power suggests QPO-like behaviour. The origin of this power is flare-like

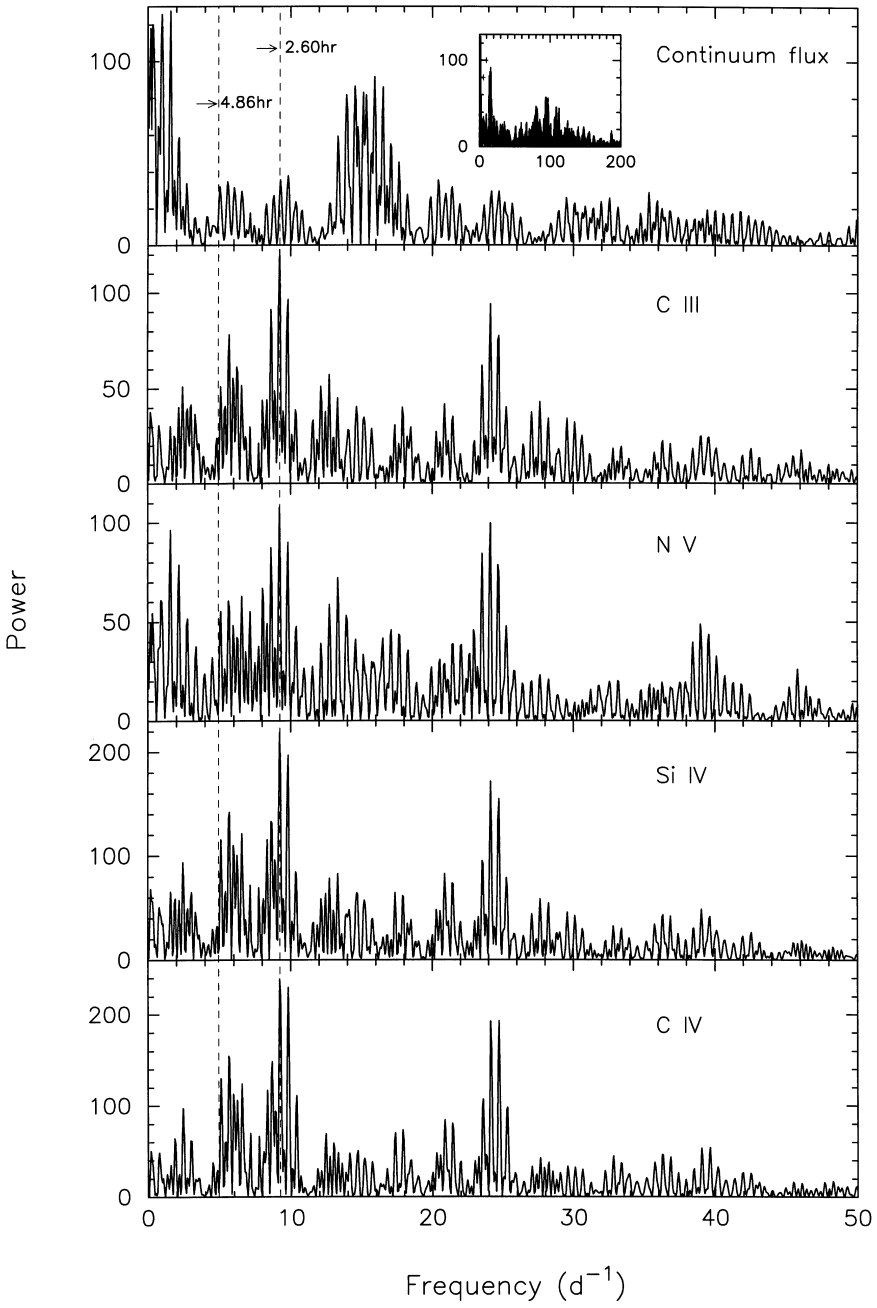

Figure 2. Fourier power spectra of time-series representing (from top to bottom) the continuum data and the fluxes beneath the C III, N V, Si IV and C IV lines. The leftmost dashed line marks the frequency of the 4.8-h period, while the rightmost dashed line indicates the frequency of the 2.6-h period. The inset in the top panel shows the Fourier spectrum of the continuum data over a wider frequency domain, highlighting the enhanced power near 96 d^{-1}.

events in the continuum light curve, typically with an amplitude of about 10 per cent. Thus, while we find no convincing evidence of coherent modulations in the FOS UV continuum data, the QPO phenomenon seems to be a persistent feature in the signal of V795 Her, affecting the X-ray, UV and optical output of the system.

Another important point is that in neither the lines nor the continuum do we find any convincing sign of the 4.8-h 'period' detected in earlier *IUE* observations (PDR; PR).

Finally, we also searched the UV continuum light curve for evidence of the 2.8-h variation which has been detected in the past in the optical light curve. We find it to be absent from these data and estimate an upper limit of about 5 per cent on the semi-amplitude of coherent modulation at this period. This is consistent with its absence from our contemporaneous optical data (Dickinson et al. 1997) and from other recent optical observations (see Patterson & Skillman 1994; Rosen et al. 1995).

3.2 Comparison with *IUE* spectra

The extensive catalogue of *IUE* spectra from V795 Her (PRS – 1989 October 12 and 13; PDR – 1990 August 6 and 7; PR – 1992 August 13-18) permits direct comparison of the UV spectrum at different epochs. In Fig. 3 we plot the 1200–1600 Å portion of two of the *IUE* SWP spectra presented by PDR, one when the C IV

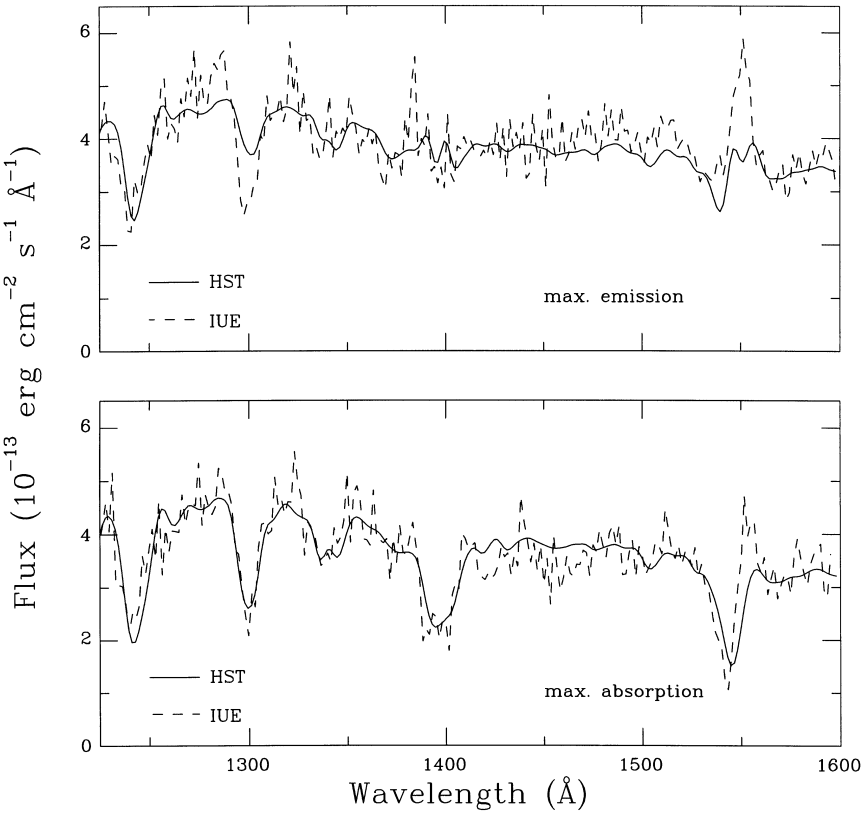

Figure 3. The two *IUE* SWP spectra of V795 Her, taken in 1990 August (see PDR), show the most extreme profiles of the C IV line, i.e. those with the most intense emission (upper panel) and deepest absorption (lower panel). Overlaid are corresponding extreme examples from our *HST* data, degraded to the same spectral resolution as the *IUE* data. The continuum levels have been normalized. Note the substantially stronger emission in the *IUE* data and the very different behaviour of the 1300-Å blend.

emission was strongest, the other when the absorption was most prominent. Superimposed on these are corresponding examples from our current HST data, degraded to the same spectral resolution as the *IUE* data. The continuum level in the *IUE* observations was ~25 per cent weaker than during the *HST* run and, accordingly, has been rescaled to match. Significant differences are evident. Prominent amongst these is the contrast in strength of the emission peak in the C IV line, which is much greater in the *IUE* data. The relatively stable 1300-Å blend in the *IUE* data also contrasts with the obvious variations exhibited in the *HST* spectra. Changes in the Si IV line are more closely matched.

3.3 The state of the system

The *HST* UV data of V795 Her presented here pose a major problem in relation to our previous *IUE* observations of the star (PRS; PDR; PR) because we now observe a strong 2.6-h variation in the lines which was not apparent in the *IUE* data. We doubt that the 4.8-h period detected instead was due to a sampling problem, given that the variation was seen in two independent data sets, both of which were long enough to establish its presence (see PR), and sampled in different ways. It is not obvious how a 4.8-h alias could have arisen in either run. It is possible that the 4.8-h 'period' might simply reflect fortuitous coverage of a non-coherent time-scale in the light curve (see also Patterson & Skillman 1994). The significance of the 4.8-h time-scale remains to be determined. If a clear 2.6-h signal had been present in the earlier *IUE* data, it is implausible that it would have escaped attention, given that the *IUE* line flux light curves folded on that period (see fig. 3 of PR) sampled it adequately and yet showed no sign of a systematic effect.

Thus we suspect that our present *HST* run found the system in a somewhat different state from the previous *IUE* runs where the 2.6-h clock may have been swamped by another phenomenon. This view is reinforced by the spectral changes reported in Section 3.2. It is worth bearing in mind that if the apparent difference in behaviour is connected to the mass transfer rate, the typical UV continuum flux level during the earlier *IUE* observations was around 25 per cent *lower* than at the epoch of the *HST* observations, suggesting that the properties of the system are quite sensitive to the accretion rate. It is interesting to note that V795 Her has exhibited odd UV behaviour in the past, as indicated by the weak-lined spectra from the first shift (1989 October 12) of *IUE* observations presented in PRS. An intriguing question that arises is whether the absence of both the 4.8-h UV and 2.8-h optical modulations (Dickinson et al. 1997) is coincidental (see also Patterson & Skillman 1994).

4 THE LINE PROFILES

We have established that in these new *HST* data the dominant variation in the UV lines occurs at the 2.6-h period. To investigate the line changes in more detail, the FOS spectra were phase-folded into 20 phase bins according to the ephemeris of Shafter et al. (1990), i.e. $T_0 = \mathrm{JD}_\odot\ 244\,7329.824 + 0.108\,2468N$, where N is the cycle number. Note that the period is incorrectly quoted in some places in the paper of Shafter et al. The epoch of this ephemeris refers to the *red-to-blue* crossing phase of the radial velocity motion

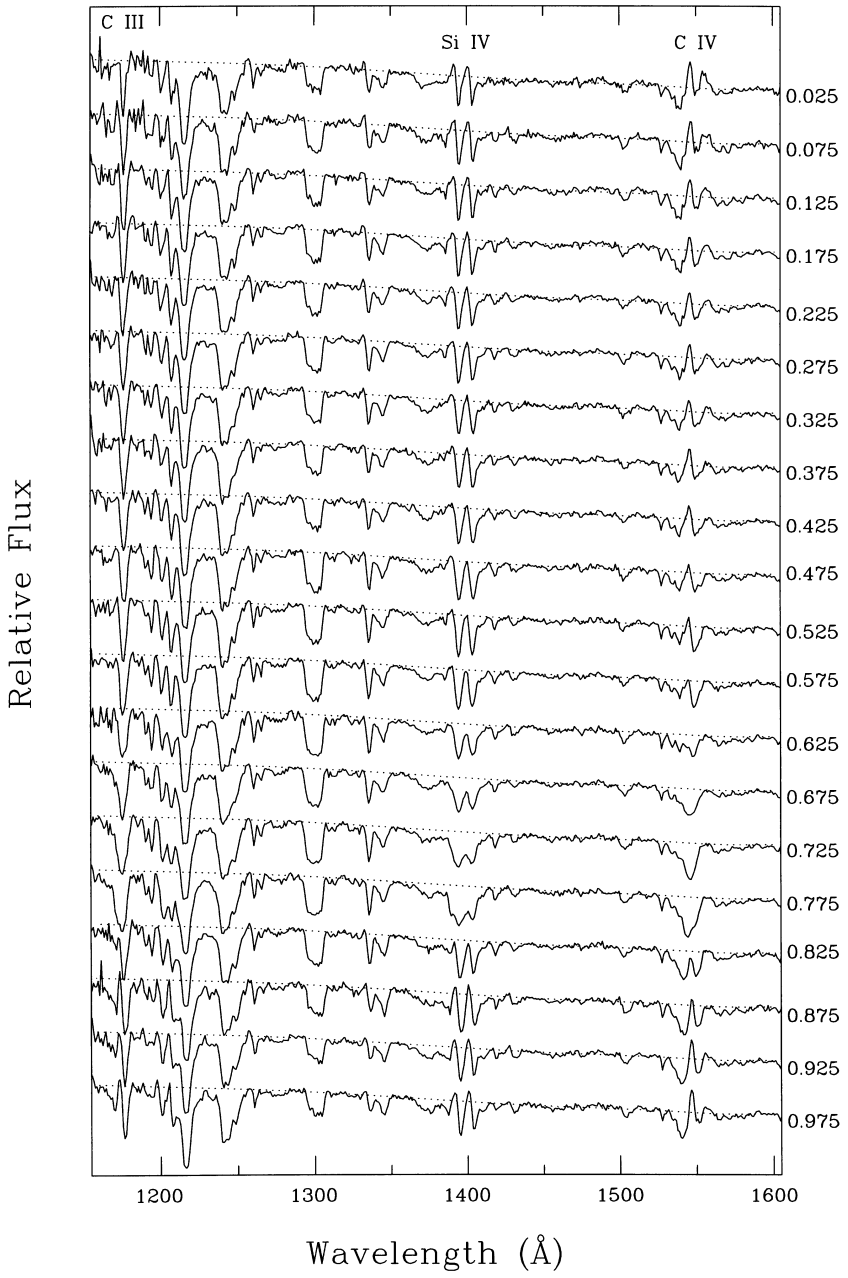

Figure 4. The phase-folded *HST* spectra (1150–1600 Å), resolved into 20 phase bins (indicated on the right). The dotted line provides a common reference level for each spectrum.

of the S-wave noted by Shafter et al. in the optical emission lines – they associated the S-wave with the orbital motion of a bright spot on the edge of the accretion disc. At the epoch of our *HST* observations, the accumulated phase uncertainty arising from the use of this ephemeris is 0.06. Fig. 4 shows, for reference, a sequence of 20 phase-resolved spectra covering the entire 1150–1600 Å range.

In Fig. 5 (opposite) we present colour-coded 'grey-scale' images for the C III, Si IV and C IV lines, trailed over the 2.60-h cycle. Being effectively a singlet, the C III line provides an important comparison with Si IV and C IV. Here, and in all other figures presented in velocity space (unless otherwise stated), zero velocity for the C IV line is aligned with the flux-weighted centroid of the doublet (assuming a flux ratio for the blue and red components of 2:1) which is at 1549.05 Å, while the zero-velocity point for the Si IV data is aligned with the bluemost (λ1393.76) doublet component.

Before discussing the phase behaviour in more detail, we first draw attention to the basic structure of the line profiles. Concentrating on the shape of the C IV line (lowest panel), one sees that the line spans the velocity range from about −3500 to +1000 km s^{-1} (or maybe even +2000 km s^{-1} if the redward bump between +1000 and +2000 km s^{-1} is a part of the C IV profile). The asymmetric, extended blue wing of the line is seen in absorption, with two shallow absorption lines owing to Si II λ1527 (−4270 km s^{-1}) and Si II λ1533 (−3110 km s^{-1}) superposed. The minimum of the deepest profile, observed at about phase 0.75, lies near −1000 km s^{-1}, but at other phases (see below) it is masked by the

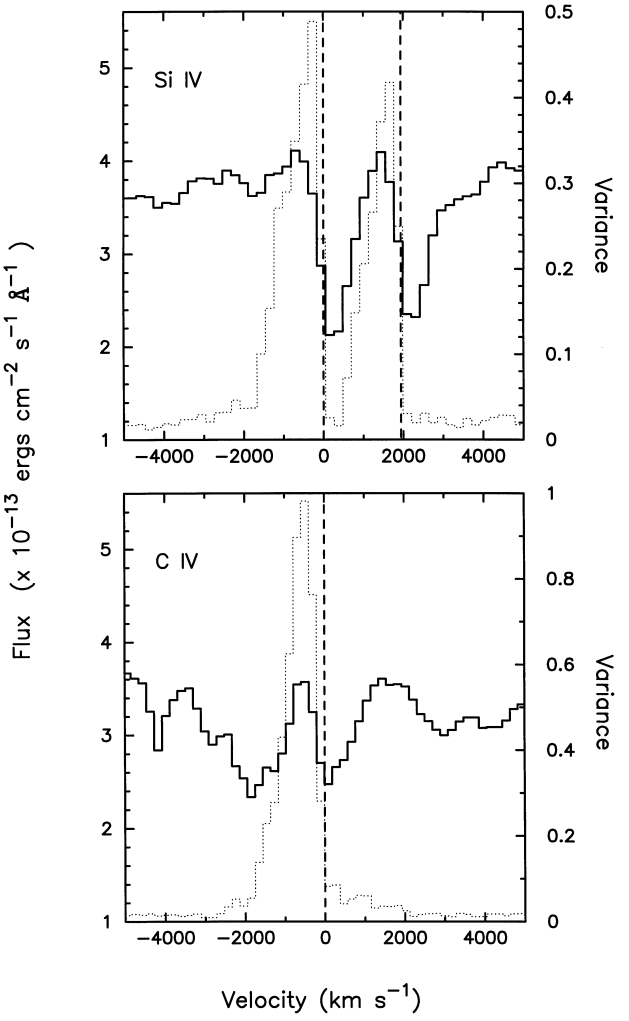

Figure 6. The top panel shows the mean Si IV line profile (solid line) (left-hand scale) and the variance profile (dotted) (right-hand scale). The vertical dashed lines mark the rest velocity of each doublet component. The velocity scale is with respect to the blueward component. The lower panel is similar but for the C IV line, and the dashed line marks the position of rest velocity for the weighted centroid of the doublet (1549.05 Å).

presence of an apparently narrow emission peak located near $-600\,\mathrm{km\,s^{-1}}$. In C III, the minimum of the deepest profile occurs near $-200\,\mathrm{km\,s^{-1}}$ but, as with C IV, for most of the cycle the blue side of the trough is filled in by an emission feature. The C III characteristics are essentially replicated in both doublet components of the Si IV line.

An idea as to which parts of the line profiles vary can be gained from Fig. 6 where the average line shapes for the C IV and Si IV lines are overlaid with the corresponding variance profiles. The variance is clearly concentrated blueward of rest velocity and, as graphically demonstrated by the C IV data, correlates very well with the emission peak.

We now consider the pattern of variation in more detail. The 'grey-scale' image of the raw C IV data (upper right panel) confirms that the most prominent changes are restricted to the velocity regime between about -1500 and $0\,\mathrm{km\,s^{-1}}$ (i.e. around the emission feature). These changes are largely confined in phase to the interval between 0.55 and 0.85 when the central emission feature (in blue) appears to fade, transforming the profile into a pure absorption trough at about phase 0.75. The extended blue absorption wing between -3500 and $-2000\,\mathrm{km\,s^{-1}}$ is broadly constant around the entire binary cycle, as is the red wing of the absorption structure in the range +500 to $+1000\,\mathrm{km\,s^{-1}}$. The redward bump that lies between about +1000 and $+2000\,\mathrm{km\,s^{-1}}$ shows modest changes near phase 0. In C III, the redward absorption trough starts to broaden at about phase 0.55, extending blueward to about $-1500\,\mathrm{km\,s^{-1}}$ by phase 0.75, before rapidly retreating to its original shape by phase 0.85. As in C IV, the red wing of the absorption trough in C III is stable throughout the cycle. The same pattern of variations is largely repeated in the Si IV line. Neither the C III nor Si IV lines show an obvious counterpart to the extended blueward absorption wing (-3500 to $-2000\,\mathrm{km\,s^{-1}}$) seen in the C IV line. The variations in each line are repeated in all three *HST* visits.

Although these *HST* data permit many possible interpretations of the line composition, for illustrative purposes we present the two extreme cases as phase-folded trailed 'grey-scale' images in Fig. 5. In the first case (central panels) we subtracted a template with the strongest emission structure (an average of phase bins 0.975, 0.025 and 0.075), pushing the residuals into absorption. The lower images show the case where we have instead subtracted a template of the deepest absorption profile (an average of spectra in phase bins 0.725 and 0.775) from all phase bins, forcing the residuals into emission. In essence, these opposing approaches reveal the cyclic pattern that arises if the changes are largely driven by variations in an absorption component (central panel) or an emission component (lower panel). We emphasize that intermediate cases (emission and absorption) are also possible. Two further aspects of the data arising from this analysis are considered below.

4.1 Comparison of the profiles at phase 0.775

In Fig. 7 are overlaid the profiles of the C III, Si IV and C IV lines observed at phase 0.775 when the line fluxes are at minimum. These profiles suggest the presence of a common absorption component. The blueward limit of this component at $-1500\,\mathrm{km\,s^{-1}}$ is obvious in the C III and Si IV lines. In the C IV line it is perhaps less evident owing to blending with an extended blueward absorption wing, but it can be identified with the shoulder at $-1500\,\mathrm{km\,s^{-1}}$. The redward limit of the trough is also well defined by the common redward shoulder in the C III and C IV lines at about $+1200\,\mathrm{km\,s^{-1}}$. A consistent limit is also measured in the Si IV line from the longward limit of the redward doublet component (which occurs around $+3100\,\mathrm{km\,s^{-1}}$ on the velocity scale of Fig. 7).

We thus conclude that all three lines harbour an absorption component between -1500 and $+1200\,\mathrm{km\,s^{-1}}$, which is most easily isolated, and cleanly characterized by the C III line shape at phase 0.775. The minimum of the C III line appears displaced blueward of rest velocity, perhaps by as much as $350\,\mathrm{km\,s^{-1}}$. The minimum of the Si IV line, as measured from a double Gaussian fit to the profile in which the component widths were held equal and the flux ratio allowed to depart from 2:1, is $-142\pm172\,\mathrm{km\,s^{-1}}$. In the case of C IV, the minimum is displaced blueward by about $800\,\mathrm{km\,s^{-1}}$, but this is most likely a consequence of blending with the extended blueward wing that only this line possesses. It is unclear whether the common absorption profile outlined here is a single structure or a superposition of two absorption components (one constant, the other variable perhaps). We return to this in Section 5.3.

We also comment on, but do not pursue, the fact that the N V and C II lines possess rather different structures at phase 0.775 from those witnessed in the other lines. For clarity, the data for these two

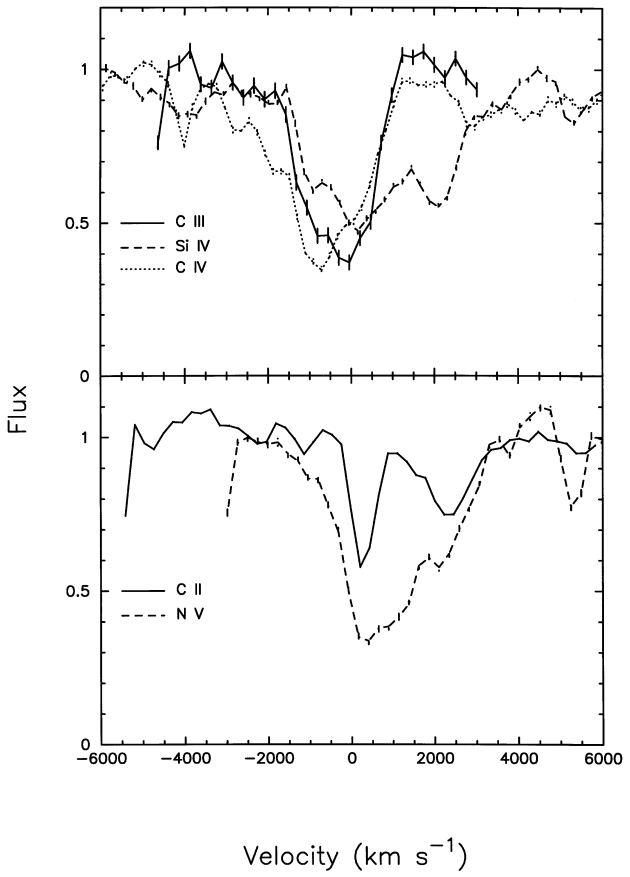

Figure 7. Upper panel: profiles of the C III (solid), Si IV (dashed) and C IV (dotted) lines from phase 0.775, normalized to the same local continuum level, and overlaid. Lower panel: a similar overlay of the N V and C II lines. Note that, here, zero velocity for the N V, Si IV and C IV doublets corresponds to the rest wavelength of the blueward doublet component in each case.

lines are presented in the lower panel of Fig. 7. The minimum in the N V line occurs near +300 km s^{-1} and the blue wing shows no evidence of the sharp truncation of the trough at −1500 km s^{-1} that is detected in the profiles of the C III, Si IV and C IV lines. The N V line is contaminated significantly on its red wing by C III λ1247 (which is seen at 2080 km s^{-1} on the velocity scale of Fig. 7). The C II line is much narrower (full width at base ∼900 km s^{-1}) than any of the lines shown in the upper panel. To make a further exploration of possible differences between lines of different ionization state, we also folded the flux curves of the lines on the 2.6-h period. While we found marginal signs that the mid-ionization lines of C IV and Si IV may reach maximum depth after the lower ionization lines (e.g. C II) by perhaps 0.05–0.1 in phase, there was no confirmation of the trend from the high-ionization line of N V or from the mid-ionization line of C III, variations for both of which are more reminiscent of that in C II.

Finally, we note that the underlying absorption profiles discussed above, and indeed the line-blanketing evident throughout the UV spectrum of V795 Her, could very well originate in a disc photosphere – see for example, Diaz, Wade & Hubeny (1996) and Long et al. (1994).

4.2 Radial velocity motion

Close inspection of the 'grey-scale' images in Fig. 5 hints at radial velocity motion within the lines, perhaps best seen in the lower panel of the C IV data where the emission feature appears to drift blueward between phases 0.9 and 1.4. To quantify this motion, we have made measurements of the C IV and C III spectra after subtraction of the line profile at phase 0.775. Measurements were not made for the Si IV line because the doublet components are partially rather than completely blended. The steps in preparation of our spectra for this measurement are shown in Fig. 8 – the example here is for phase 0.025.

We used a simple measure, the weighted centroid, to determine the line velocity. In the case of C IV, we included data in the range 1539–1560 Å (−1950 to +2120 km s^{-1}), the velocity being referenced to a weighted rest wavelength of 1549.05 Å for the unresolved doublet. For C III, the centroid was deduced using data between 1169 and 1177 Å. The results are shown in Fig. 9 and Table 1. Uncertainties were deduced after scaling the data errors so as to normalize the reduced χ^2 to 1.0.

As evident in Fig. 9, there is a discrepancy between both the amplitude and mean velocity of the motion inferred from the C III and C IV lines. However, this outcome depends on whether the redward extension (see Section 4 and Fig. 4) (1554–1560 Å, i.e. ∼1000–2100 km s^{-1}) of the C IV line is included. Table 1 (case B) demonstrates that restricting the measurement domain for this line to the range 1539–1552 Å (−1950 to +570 km s^{-1}), i.e. omitting the redward extension of the C IV line, brings the velocity amplitude into broad agreement with that seen in C III. The remaining mean velocity offset of about 90 km s^{-1} might, however, be all but accounted for if the flux ratio of the C IV doublet was closer to the optically thick value of 1:1 than the adopted 2:1 (the limiting effect would be to shift the mean motion of the C IV line blueward by about ≈80 km s^{-1}). While the emission peak is undoubtedly, and substantially, blueshifted, the reality of the radial velocity modulation is less certain. Some of the profiles (e.g. around phase 0.025) show slightly asymmetric shapes which may reflect a multi-component structure. If so, simple experiments with as few as two independent components show that the radial velocity motion could be accounted for by uncorrelated changes in the intensities of the components.

We also searched for evidence of radial velocity motion in the simpler, pure absorption-line profiles. Specifically, we investigated the absorption line at 1345 Å and the pair of features at 1419 and 1430 Å via a cross-correlation technique. While the results of the cross-correlation analysis on the latter two lines (supported by Gaussian fitting to the 1419 Å feature) suggest a small 2.6-h radial velocity modulation with a semi-amplitude of 95±57 km s^{-1} and a blue-to-red crossing phase of 0.83±0.1, we could find no corroborating motion in the 1345- Å line.

5 DISCUSSION

In the preceding sections, we have described the basic temporal and spectral properties of the UV spectrum of V795 Her apparent in our *HST* observations. The behaviour of the source is different from that during our earlier *IUE* studies, with the dominant time-dependent phenomena now being tied to a 2.6-h rather than a 4.8-h period. One implication of these *HST* observations is that, if the 2.6-h period were the binary period, they would place V795 Her back amongst the more conventional non-magnetic cataclysmic variables where UV line variations, when detected, are on the binary period (for example, see Drew 1993). In this section, we consider possible interpretations of the line profiles. We begin by commenting briefly on the extended blueward wing of the C IV line.

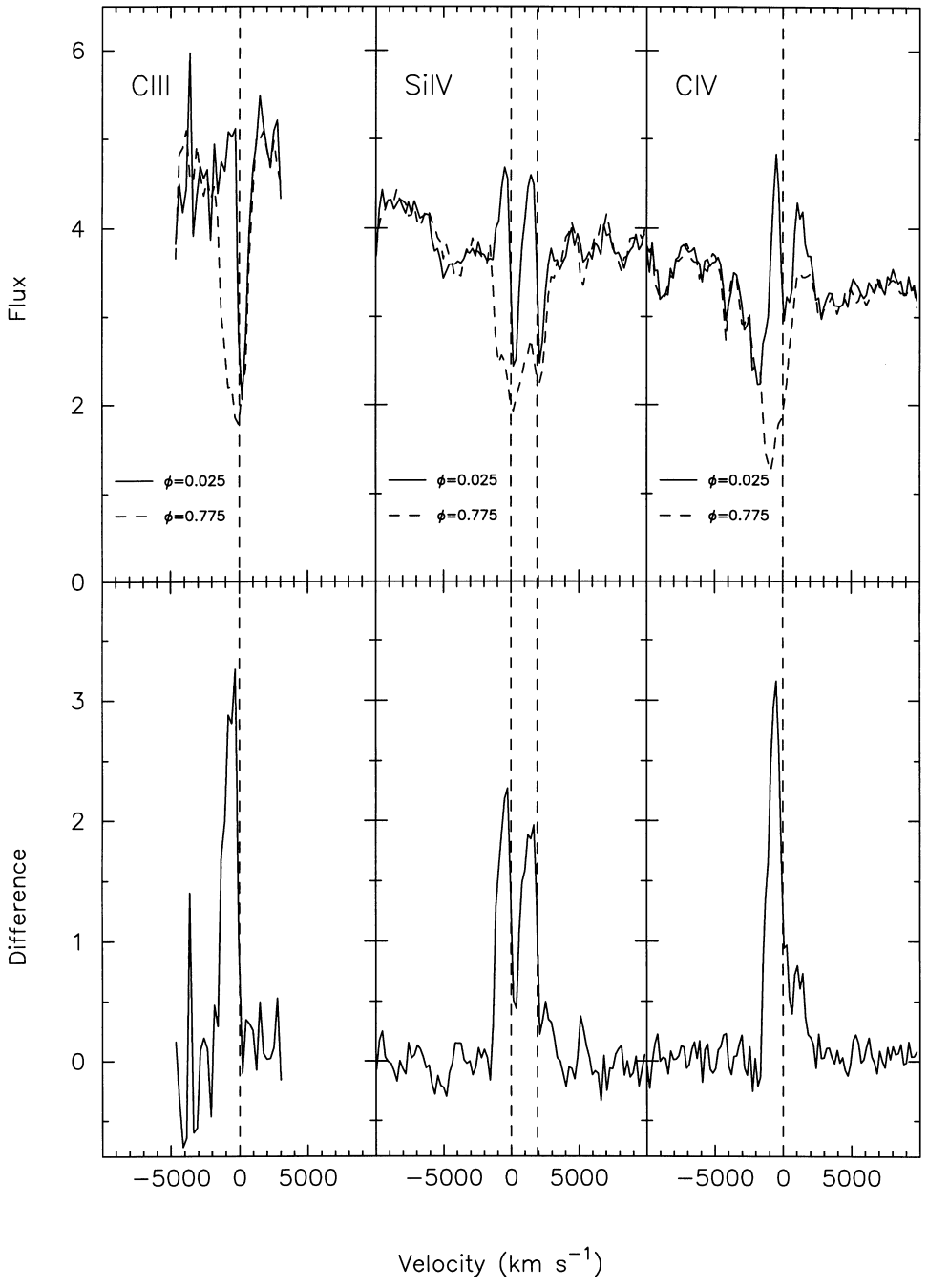

Figure 8. The upper panels show an overlay of the C III, Si IV and C IV line profiles from phases 0.025 (solid) and 0.775 (dashed). Note that to remove cycle-to-cycle variations in the overall flux level, the spectra in these plots have been normalized to the same level via comparison of 'continuum' regions adjacent to each line. The lower panels show the corresponding difference profile which in each case is dominated by an emission component. The dashed vertical lines indicate the rest velocities of the lines (for C IV, it is for the weighted centroid of the doublet).

5.1 The high-velocity C IV absorption component

The asymmetric, blueward absorption trough is present at all phases in the C IV line and can be traced shortward of -1500 km s^{-1} to perhaps -3500 km s^{-1}. It is, however, difficult to determine the blueward limit of the C IV absorption wing, owing to the effects of line blanketing and more distinct absorption lines, notably at about -4000 km s^{-1} (1527 Å). This line and the less prominent feature at -2750 km s^{-1} (1534 Å) are presumably due to Si II λ1526.7 and Si II λ1533.5. The extended C IV absorption component, which we associate with a fast wind outflow in V795 Her, has no obvious counterpart in the Si IV or C III lines. The relative stability of the C IV profile between -3500 and -2000 km s^{-1} suggests that any asymmetry in the wind outflow is small or viewed at low inclination.

5.2 A narrow-emission-line interpretation?

We demonstrated in Section 4 that the dominant variations in the lines are confined to the domain of the 'emission peak'. This feature is present in each of the three lines studied in most detail, but is most

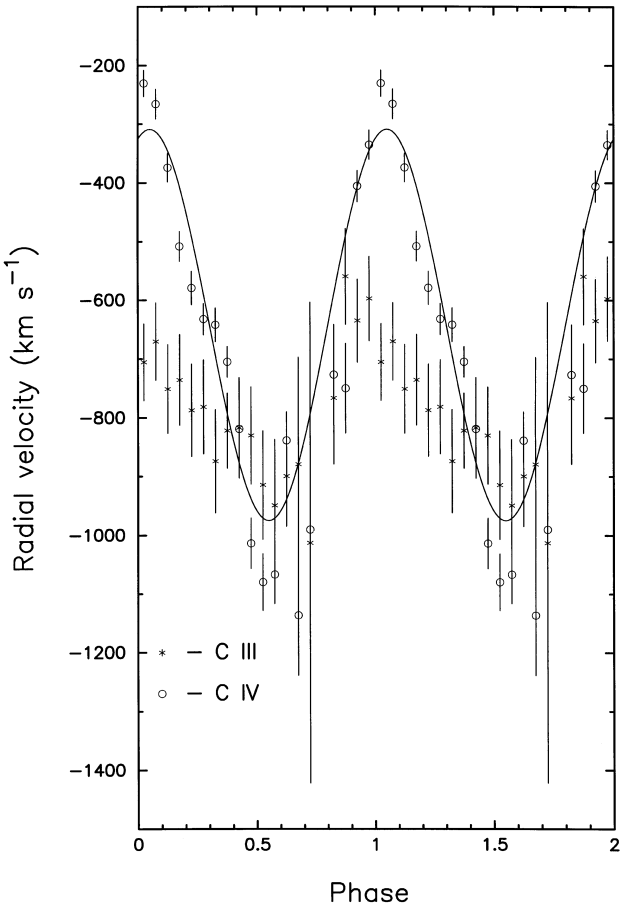

Figure 9. The radial velocity motion of the effective centroid of the emission peak in the C III line (stars) and C IV line (circles). The C IV data represent measurements that include data in the range 1539–1560 Å, i.e. incorporating the redward extension on the C IV line. The solid curve is the best-fitting sine wave to the C IV data.

Table 1. The mean velocity (V_m), semi-amplitude (V_a) and blue-to-red crossing phase (ϕ_0) derived from measurements of the radial velocity motion of the emission peaks in the C IV and C III lines. In case (A) for the C IV line, data between 1539 and 1560 Å were used (i.e. the redward bump is included). In case (B), the redward bump was omitted from the analysis.

Line	V_m (km s^{-1})	V_a (km s^{-1})	ϕ_0
C IV(A)	−640±50	330±60	0.80±0.04
C III	−770±40	120±50	0.73±0.09
C IV(B)	−670±30	160±35	0.76±0.05

clearly identified in C IV where the extended blueward absorption structure helps to separate it, visually, from the local continuum. Most simply, the appearance and variation of the profiles suggest that a narrow emission component (FWHM∼1000 km s^{-1}) is primarily responsible for the changes seen. These occur mainly in the short interval between phases 0.55 and 0.85, during which the emission fades away gradually to a minimum at phase ∼0.775 and then recovers rapidly. Significantly, this emission peak is indisputably blueshifted to a mean radial velocity of around −600 km s^{-1}.

If correctly identified as a narrow emission feature, this component poses a severe challenge to any conventional source of emission within the system. In disc-accreting binaries, one location often invoked to explain narrow, low-velocity-amplitude optical emission-line features is a bright spot where the infalling stream from the secondary star interacts with the outer disc. One might be tempted to associate the narrow UV emission feature in V795 Her with a putative bright spot – note there is no reliable information on the phasing of inferior conjunction of the secondary star in V795 Her. However, the mean motion of the bright spot should reflect the systemic motion. In V795 Her, the ∼600 km s^{-1} net blueshift of the UV emission feature is implausibly large and is discrepant with the roughly centred locations of the optical emission lines – there is no obvious optical counterpart to the UV emission peak. The width of the feature is also somewhat larger than might be expected for material circulating at the edge of the disc.

Another hypothetical source for the narrow emission peak would be part of an infalling stream that overflows the disc edge and re-impacts closer to the white dwarf (e.g. Armitage & Livio 1996, and references therein). The lack of substantial radial velocity excursions essentially rules out the possibility that we could be viewing such overflow at large inclinations. Appealing to a low-inclination scenario is not convincing either. The blueshifted motion would imply an upwardly directed flow, but it is unlikely that this could come from the initial deflection of the overflowing stream after impact with the disc edge, since the deflection angle is believed to be very small. Whether the re-impact of the stream near the inner disc could produce a splash-back with sufficient vertical motion is uncertain (and untested), but in any case it is unclear why we would see only the splash-back in emission and no sign of the subsequent infall. It must be remembered that one also needs either to hide the emission source and/or to introduce compensating absorption over the same velocity regime to account for the decline of the feature around phase 0.75.

We conclude that, while it is tempting to attribute the 2.6-h changes of the UV lines in V795 Her to a narrow emission component, we are not yet able to find a convincing source within the binary that could account for its observed properties. An alternative interpretation is considered in Section 5.3.

5.3 Competing models

Two models have recently been floated to explain the apparent double S-wave in the wings of the optical emission lines in V795 Her (Casares et al. 1996; Dickinson et al. 1997; see also Haswell et al. 1994). The first, propounded by Casares et al. (1996), employs a hybrid magnetic model in which a magnetic white dwarf, accreting material from a disc, rotates synchronously with the binary, the orbital period of which is assumed to be 2.6 h. Here the double S-wave is associated with emission from material diverging to feed two magnetic poles, but flowing in opposite directions along the same magnetic field line rather than, as might naïvely be expected, along azimuthally opposed field lines. Overlooking the dynamical objections raised by Dickinson et al. (1997), a significant concern for such a magnetic model is the lack of an obvious 2.6-h pulse in the soft X-ray flux from the star (Rosen et al. 1995).

In rejecting the model of Casares et al., Dickinson et al. (1997) advanced a stream overflow picture for V795 Her in which the optical double S-wave is explained as a single, broad emission component, the core of which is depressed by strong, superposed, comoving absorption. This model is similar to that proposed by

Hellier & Robinson (1994) to explain the behaviour of the optical lines in SW Sex stars. The broad emission component is believed to arise from the fast-moving material where it re-impacts with the disc, while the variable absorption comes from the stream overflowing the outer portions of the disc. Several substantial problems remain with this model, as discussed in Dickinson et al. (1997), but its basic tenets do at least provide a qualitatively plausible explanation of the underlying optical line behaviour.

We now consider whether aspects of our *HST* UV data from V795 Her might be reconciled with the basic overflow model. A simple model that could explain both the optical and UV line behaviour would be encouraging, although one must bear in mind that we are generally considering lines in the UV which are considerably more highly ionized than the optical lines. If an overflowing stream is a correct explanation of the optical line behaviour, it is likely that parts of it could also produce broadly similar UV phenomena, even though the UV absorbing and emitting sites may not be coincident with the optical ones.

Although a broad emission component is not obvious in the *HST* data, it is not necessarily surprising, since it is not obvious in the optical lines either owing to suppression of the core by absorption – its possible presence there was inferred from the wings of the lines. In a crudely similar way, it may be possible to explain the UV lines in terms of a broad emission structure (with a FWHM $\sim$1300–2000 km s^{-1}) which masquerades as the narrow blueshifted emission peak owing to the presence of absorption components that cut into its wings, mainly on the red side in C III and Si IV but on the blue side too in C IV, i.e. the wind-formed blueward absorption structure. Subtle hints that a broad feature might be present in the UV lines come from the bump that is most prominently seen just redward of the C IV line (around +1000 to +2000 km s^{-1}), particularly noticeable around phase 0.0 before it fades away around phase 0.5, and the filling-in of the region between -1000 and -2000 km s^{-1} (blueward of the peak) in the C III and Si IV lines around phase 0.3–0.6. Both are qualitatively consistent with the blueward migration of a broad emission feature between phases $\sim$0.1 and 0.5. In addition to circumventing the need to explain the bump redward of C IV, a perceived advantage of invoking a broad emission component is that its mean position is located closer to rest velocity than for the narrow-emission-peak case.

An important point to bear in mind here, however, is that it is not possible to reproduce the line profiles observed between phases 0.875 and 1.525 solely by superimposing a broad, variable emission component on the absorption structure seen at phase 0.775. The narrowness and blueshifted nature of the peaks in the variance profiles (Fig. 6) are also inconsistent with the notion that the profile variability could be produced by uniform changes in a broad emission component. We conclude that, if the lines do contain a broad emission feature, the transformation observed between phases 0.55 and 0.875 is dominated not by changes in that component, but by changes in an additional absorption component that spans the velocity regime between ~ -2000 and 0 km s^{-1} and which is effective only during that phase interval. This variable absorption could not, however, arise from a geometric asymmetry or absorption enhancement in a wind outflow, since it is tied to the 2.6-h period which is far longer than the radial transport or rotational time-scale for the outflow.

Another problem is that, although the complex UV line profiles make it difficult to quantify any radial velocity motion of a putative broad emission component, simple simulations suggest that it would be difficult to accommodate any motion that was as large as that ($\sim$400 km s^{-1}) inferred from the optical data. In particular, one would expect any substantial motion to affect significantly the shape of the red absorption wing (between 0 and 1000 km s^{-1}), contrary to the observations. The stability of the latter component suggests that a relatively invariant absorption structure is present, centred near rest wavelength. This could be associated with absorption in a disc photosphere.

To investigate further a possible connection between the UV and optical data, we derived light curves as a function of velocity through the C IV and Hβ lines. The results, shown in Fig. 10, provide some evidence of correlated behaviour. Over the velocity range $-1500 \lesssim v \lesssim 0$ km s^{-1} the C IV line shows a deep trough around phase 0.75, i.e. when the narrow emission peak disappears – the optical S-waves are at maximum blueshift then. The Hβ line also shows a flux dip near this phase, at least for data in the range $-1000 \lesssim v \lesssim 0$ km s^{-1}. On the red side of line centre, however, while flux between 0 and 500 km s^{-1} in the Hβ line shows a strong modulation that reaches a minimum near phase 0.4, and even earlier in the $500 \leq v \leq 1000$ km s^{-1} bin (i.e. in approximate anti-phase with the variation on the blue side), there is no corresponding effect in the C IV line.

In the interpretation proffered for the optical line behaviour (Dickinson et al. 1997), the flux variation is attributed mainly to the absorption component (that overlies and moves with the broad emission component) as it traverses the velocity window over which the line flux is measured. This would explain the basic, roughly anti-phased behaviour of the Hβ flux either side of the rest velocity. In the context of this model, the additional absorption invoked to account for the loss of the narrow blueshifted emission peak in the UV lines at phase 0.75 may no longer be a distinct component, but merely the UV counterpart of the optical absorption component as seen when it is near maximum blueshift. However, the model does not transfer directly to the UV lines, since we do not see the same behaviour on the red side of the line. In the UV lines, the absorption must be more variable, being strong around phase 0.75 and much weaker when redshifted at early phases in the cycle. We also face the problem that the variable absorption which affects the UV lines cuts in when the putative broad emission component is near maximum blueshift (phase 0.55–0.875), and then seems to go away. In SW Sex stars, such behaviour may be connected with the presence of a flared accretion disc, the system inclination and flare geometry conspiring to hide the absorbing portion of the stream when flowing away from the observer (Hellier, private communication). However, this probably only works for high-inclination systems, and there is no evidence to date (e.g. eclipses) that V795 Her is sufficiently inclined.

In summary, there remain many problems with the stream overflow explanation for the optical and (especially) the UV line behaviour in V795 Her which will demand quantitative assessment if the overflow model is to be a serious contender.

5.4 Variability in V795 Her compared with a T Tauri star

We end by looking at some points of similarity between the behaviour of the UV lines in V795 Her and the Balmer lines in the spectrum of the classical T Tauri star SU Aurigae. As a young enough stellar object, SU Aur is still experiencing some accretion from a circumstellar disc. As such it might be reasonable to draw some parallels between it and V795 Her . This star has been the subject of an intensive optical spectroscopic monitoring campaign (Johns & Basri 1995) that has resulted in a characterization of the pattern of variability as a function of projected velocity within the

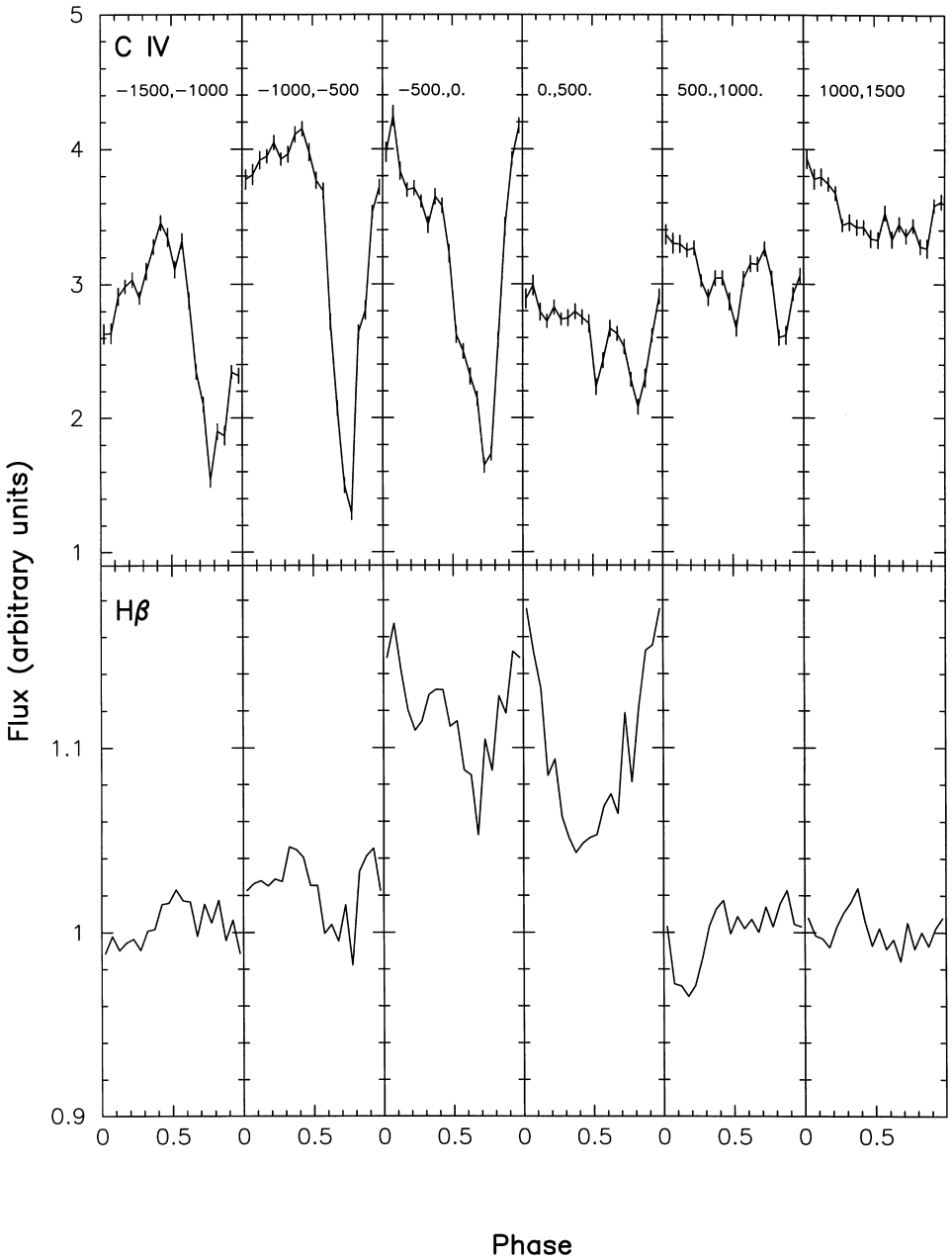

Figure 10. Light curves of the C IV (top) and Hβ (bottom) lines as a function of velocity within the line profile. Velocity bin boundaries are given in each panel. Fluxes are inclusive of the continuum level.

Hα and Hβ line profiles. It has been found that Hα varies within its blue wing on a period that matches the star's rotation period of $\sim$3 d. A similar effect is seen in the more transparent Hβ line, where anti-phased variations are also apparent in the red wing.

Johns & Basri (1995) have proposed that the pattern of variation seen in SU Aur is consistent with what they refer to as an 'egg-beater' model. The accreting star and disc are in an intermediate polar configuration wherein the magnetic axis of the star is at an angle with respect to the stellar rotation and disc axis. At the inner edge of the disrupted disc, the flow divides between a magnetically channelled accretion flow on to the star and a centrifugally driven outflow (e.g. Shu et al. 1994). The inclination of the magnetic axis breaks the axisymmetry and makes it inevitable that variation is seen on the stellar rotation period. The blue wing variations in Hα are attributed to the changing aspect of the stronger outflow associated with the inner disc edge visible to the observer to one side of the rotation axis, while the anti-phased red wing variations in Hβ are due to the stronger accretion flow on the other. The failure to detect red wing variability in Hα is very plausibly an optical depth effect.

The gravitational potential near the accreting star in a system such as V795 Her is significantly deeper than in a T Tauri object. For this reason one might expect phenomena apparent in the optical in an object such as SU Aur to shift to at least the ultraviolet in V795 Her. Could the blue wing variations seen in Hα in SU Aur be analogous to those that we have described here in C III, Si IV and C IV in V795 Her? The absence of obvious anti-phased red wing changes is not a problem in that these lines, like Hα in SU Aur, are very

probably significantly opaque. A key consideration for the analogy seems to be the significance of the 2.60-h periodicity in V795 Her, in that the analogy can only apply if this time-scale is identified with the white dwarf rotation rather than with the binary orbit. As argued by Dickinson et al. (1997), synchronism between the white dwarf spin and binary orbit seems implausible. We therefore have to conclude that this hypothesis can only be appropriate if the orbital period of V795 Her is not 2.60 h.

Whether this picture is viable remains to be established. If a disc is present, a centrifugally driven outflow would require that the magnetospheric radius, $R_{\rm mag}$, lie beyond the corotation radius, $R_{\rm co}$ – otherwise the circulating disc material would exert a spin-up torque on the white dwarf. However, for a white dwarf rotation period of 2.6 h, the corotation radius would already lie close to the edge of any disc that could comfortably fit inside a binary with a period of less than about 6 h. This suggests that if the condition $R_{\rm mag} > R_{\rm co}$ holds in V795 Her, either it is unlikely to possess a conventional Keplerian accretion disc, or the binary period is substantially longer than 6 h. Moreover, in the absence of a magnetic interaction between the stellar components, it is hard to see why the white dwarf has not already been spun up to a much shorter period than 2.6 h, unless either the binary period is very long ($\sim$ 1 d) in which case we might hope to have seen evidence of an evolved secondary star, or we have caught the system in a short-lived ($\sim 10^5$ yr) era in its life during which this spin-up is taking place.

A caveat to this discussion arises if there is magnetic coupling between the stars. Recent work examining the relation between the orbital and spin periods in the intermediate polar EX Hya (King & Wynn 1998) shows that a slowly rotating white dwarf can exist in a system the orbital period of which is a factor of a few longer than the spin period. Here there is no conventional accretion disc. The infalling material from the secondary star interacts directly with the white dwarf field and can lead to episodes of accretion and ejection on the spin period which depend on the orientation of the field with respect to the companion star. In this context, it is worth noting that spin-phase-dependent absorption on the blue side of the C IV line may also have been seen in *HST* observations of EX Hya (Stavroyiannopoulos et al., in preparation; Long, private communication). If V795 Her is similar, we might anticipate an orbital period of 4–8 h, perhaps raising speculation about the origin of the 4.8-h periodicity in the *IUE* data. However, the lack of reported phenomena at this period in other wavebands might weigh against such a notion. One would also have to consider whether the optical behaviour in V795 Her were compatible with this picture and, perhaps more importantly, whether one could explain the apparent lack of a prominent 2.6-h X-ray modulation. Nevertheless, the *HST* results, when considered alongside the broadly analogous behaviour seen in SU Aur and perhaps EX Hya, will ultimately have to be weighed against the prevailing view that the binary period of V795 Her is 2.6 h. It also seems that a magnetic scenario for V795 Her has yet to be laid to rest.

6 CONCLUSIONS

We have presented highly time-resolved *HST* UV spectroscopy of the nova-like binary V795 Her. The 4.8-h variation detected in the line fluxes during earlier *IUE* observations is no longer evident, being replaced by a strong signal at the 2.6-h period. This change in temporal behaviour, which seems to be accompanied by changes in the line spectrum, suggests that the *HST* observations caught the system in a rather different state from our earlier *IUE* observations. While no coherent pulse is detected in the UV continuum, a $\sim$15-min QPO-like phenomenon, similar to that seen in earlier optical and X-ray light curves, is present.

The least contentious feature of the UV lines is the asymmetric blueward absorption trough which is seen only in the C IV line. We associate this structure, which is approximately constant throughout the binary cycle, with an outflowing wind. However, it is relatively weak and partially blended with time-variable structures in the line core.

The 2.6-h variation in the lines is restricted to a narrow velocity range between about -1500 and 0 km s^{-1}, i.e. concentrated almost exclusively on the blue side of the line. Naïvely, a variable, narrow, blueshifted emission component provides the most obvious explanation for the 2.6-h cycle in the C III, Si IV and C IV line profiles. However, we cannot identify a convincing source within the system that could account for its highly blueshifted velocity and flux variability. We examined the UV data for signs that a self-absorbed, broad emission component might be present in the lines, as proposed to explain the optical data presented by Dickinson et al. (1997) where it was tentatively associated with stream overflow of the disc. There is some circumstantial evidence that a broad component may contribute to the UV lines, but we are not able to isolate it reliably. If a broad component is present, it appears that a phase-dependent, blueshifted absorption component is also needed to account for the gross 2.6-h line variability. Nevertheless, several qualitative and quantitative problems remain with the basic overflow picture, and a convincing model for the system remains elusive. In addition, it seems that the line profiles contain a broadly phase-stable absorption component which, along with clear signs of line blanketing across the UV spectrum, indicates that absorption, perhaps in a disc photosphere, is an important component in the lines of V795 Her.

Finally, we note some similarities between the velocity-restricted changes in the lines of V795 Her and the optical lines of some T Tauri stars. Related behaviour may also have been observed in UV data from the intermediate polar EX Hya. In T Tauri systems at least, the variability may be associated with magnetically controlled inflows and outflows tied to the rotation of the central star. If evidence of a link between V795 Her and T Tauri stars (and perhaps EX Hya) is eventually confirmed, we will need to revisit the question of whether the 2.6-h period is really orbital, and indeed whether V795 Her is truly distinct from intermediate polars.

ACKNOWLEDGMENTS

We are grateful to Richard Wade for providing us with a number of model disc spectra. Partial support for this work was provided by NASA through grant number GO-5362 to SBH from the Space Telescope Science Institute, which is operated by AURA, under contract NAS5-26555.

REFERENCES

Armitage P. J., Livio M., 1996, ApJ, 470, 1024
Baidak A. V., Lipunova N. A., Shugarov S.Yu., Moshkalev V. G., Volkov I., 1985, Inf. Bull. Variable Stars, No. 2676
Bohlin R., 1995, in Koratkar A., Leitherer C., eds, Calibrating Hubble Space Telescope Post Servicing Mission. ESO, p. 49
Casares J., Martinez-Pais I. G., Marsh T. R., Charles P. A., Lázaro C., 1996, MNRAS, 278, 219
Dahlem M., 1995, in Koratkar A., Leitherer C., eds, Calibrating Hubble Space Telescope Post Servicing Mission. ESO, p. 72
Diaz M., Wade R., Hubeny I., 1996, ApJ, 459, 236

Dickinson R., Prinja R. K., Rosen S. R., King A. R., Hellier C., Horne K., 1997, MNRAS, 286, 447
Drew J. E., 1993, in Regev O., Shaviv G., eds, Proc. 2nd Technion Haifa Conference, Ann. Israel Phys. Soc., Vol. 10, Cataclysmic Variables and Related Physics. Israel Physical Society, p. 128
Haswell C. A., Horne K., Thomas G., Patterson J., Thorstensen J. R., 1994, in Shafter A. W., ed., ASP Conf. Ser. Vol. 5, Interacting binary stars. Astron. Soc. Pac., San Francisco p. 268
Hellier C., Robinson E. L., 1994, ApJ, 431, L107
Johns C., Basri G., 1995, ApJ, 449, 341
Kaluzny J., 1989, Acta Astron., 39, 235
King A. R., Wynn G. A., 1998, MNRAS, in press
Koratkar A., Evans I., 1995, in Koratkar A., Leitherer C., eds, Calibrating Hubble Space Telescope Post Servicing Mission. ESO, p. 78
Long K. S., Wade R. A., Blair W. P., Davidsen A. F., Hubeny I., 1994, ApJ, 426, 704
Mironov A. V., Moshkalev V. G., Shugarov S.Yu., 1983, Inf. Bull. Variable Stars, No. 2438
Patterson J., Skillman D. R., 1994 PASP, 106, 1141
Prinja R. K., Rosen S. R., 1993, MNRAS, 262, L37 (PR)
Prinja R. K., Rosen S. R., Supelli K., 1991, MNRAS, 248, 40 (PRS)
Prinja R. K., Drew J. E., Rosen S. R., 1992, MNRAS, 256, 219 (PDR)
Rosen S. R., Branduardi-Raymont G., Mason K. O., Murdin P. G., 1989, MNRAS, 237, 1037
Rosen S. R., Watson T. K., Robinson E. L., Prinja R. K., Misselt K., Shafter A. W., 1995, A&A, 300, 392
Shafter A. W., Robinson E. L., Crampton D., Warner B., Prestage R. M., 1990, ApJ, 354, 708
Shu F., Najita J., Ostriker E., Wilkin F., Ruden S., Lizano S., 1994, ApJ, 429, 781
van Teeseling A., Beuermann K., Verbunt F., 1996, A&A, 315, 467
Zhang E., Robinson E. L., Ramseyer T. F., Shetrone M. D., Stiening R. F., 1991, ApJ, 381, 534

This paper has been typeset from a TEX/LATEX file prepared by the author.